

A new technique for multi-cell joint channel estimation in time division code division multiple access based on reduced rank singular value decomposition

Ali K. Marzook · A. Ismail · B. M. Ali ·
A. Sali · S. Khatun

Published online: 19 September 2013
© Springer Science+Business Media New York 2013

Abstract A new technique for multi-cell joint channel estimation (MCJCE) in time division code division multiple access based on singular value decomposition (SVD) reduced rank technique is proposed in this paper. MCJCE is one of the effective solutions to improve the mobile system performance throughout mitigate the inter-cell interference from the neighboring cells. The increasing complexity of multi-cell system model due to the additional processing of the interferer users will be solved by using SVD reduced rank technique, where a limited number of parameter that really need it to describe the channel matrix will be estimated. Two models of multi-cell approaches are discussed, the first one depended on reconstruct the convolutional midamble matrix of inactive users in serving cell by the strongest interferer users from the neighboring cells. The second one will be more inclusive to user traffic scenarios in mobile systems and will be expanding to contain all detected users. The simulation results prove the validity of the proposed reduced rank technique for precision channel estimation (6.4 and 5 dB) and (9 and 7 dB) for case 1 and 2 respectively; BER performance improvements over the conventional estimators.

Keywords TD-SCDMA · Joint channel estimation (JCE) · Multi-user joint detection (MUJD) · Reduced rank techniques · SVD

1 Introduction

TD-SCDMA has been classified as one of 3G wireless communication systems. The physical layer of this system has adopted several advanced technologies, such as: joint detection, uplink synchronization, and smart antennas [1]; making it capable of meeting the requirements of 4G systems directly. Over the last years, TD-SCDMA has gained a great attention in research and industry applications. In addition to being one of the most prevalent cellular systems, it has been associated with many other applications, such as: Wireless Sensor Network (WSN), mobile Internet of things networks, and monitoring the production condition exactly and in a real-time manner under the ground and surface of coal mine [2, and their references].

The physical layer of TD-SCDMA system can be viewed as a three dimensional structure, where it can manipulate data of a specified carrier frequency, time slot, and signature code. Therefore, it allows the processing of K_{max} users located in the same serving cell at the same time slot in the uplink and/or downlink directions. However, cellular system that implements TD-SCDMA as a platform suffers mainly from the appearance of Inter-symbol Interference (ISI), intra-cell Interference, and inter-cell interference (ICI). ISI is an inherent feature of this system as the frequency-selective channel has a delay spread in the order of symbol interval. Intra-cell interference or Multiple Access Interference (MAI) arises due to the fact that there are K users in the same time slot and when only one user is intended to be detected, the remaining $K - 1$ users acts as

A. K. Marzook (✉)
Petroleum Engineering, Faculty of Engineering,
University of Basrah, Basrah, Iraq
e-mail: akmarzook@iee.org

A. K. Marzook · A. Ismail · B. M. Ali · A. Sali
Computer and Communication Systems Department,
Faculty of Engineering, Universiti Putra Malaysia, Serdang,
Malaysia

S. Khatun
Faculty of Computer Systems and Software Engineering,
Universiti Malaysia Pahang, Gambang, Pahang, Malaysia

an interference. Single cell multi-user joint detection (SC-MUJD) equalizers are a preferred option in eliminating MAI. The suboptimal linear equalizers: zero forcing-block linear equalizer (ZF-BLE) and minimum mean square error-block linear equalizer (MMSE-BLE) are repeatedly employed at the receiver to suppress ISI, MAI, and jointly detect data of the K users [3]. At last, Inter-cell interference arises from users in the adjacent cells and may be mitigated by implementing Multi-Cell-MUJD (MC-MUJD) equalizer techniques [4]. The suggested MC-MUJD equalizers in the previous works are a modified version of SC-MUJD equalizers; hence data of inactive users in the serving cell are replaced by those of interfering users from neighboring cells to permit joint detection [5].

In practical situations, the huge demand on the services with high density areas forced the optimizers of the mobile communication systems to increase the system capacity by sharing the same time slot for many users. The using of multi-cell channel estimation bring very important enhancement and improving in channel estimation part, while require estimating many channel parameters for the adjacent interferer users, where each added user has a different channel impulse response with different amplitude and relative delay. The processing time will increase tremendously due to the additional process for each user, or the complexity of the whole system will be increased due to adding support hardware. That will lead to a significant degrade in the system performance.

All the aforementioned equalizer types require the computation of an accurate version of Channel Impulse Response (CIR) for all the intended users. Several approaches have been proposed for single cell-joint channel estimation (SC-JCE), such as: Least Square (LS), B. Steiner, and minimum mean square error (MMSE) estimators [5]. For Multi-cell case, the LS and MMSE estimators are extended to handle Multi-Cell-JCE (MC-JCE) for the active users in the serving cell and strong interferes [6]. The extension of previous works was based on omitting inactive users from the serving cell total midamble matrix \mathbf{G}_{sc} and inserting the midamble convolution matrices of the strong interferes. However, both single-cell and multi-cell CIR estimators steer high computational algorithms, which attempt to calculate a high number of parameters during a short length of training sequences. Accordingly, the resulting estimation and recovered data have a significant deviation from the actual solutions. The suggested method in this paper overcome the above mentioned constraints is to parameterize the total full rank temporal channel matrix \mathbf{H} of TD-SCDMA systems in terms of parsimonious representation. This can be achieved if a reduced rank model is exploited for matrix \mathbf{H} ; causing a considerable reduction in the number of its coefficients that requisite to be estimated. The rank deficiency of \mathbf{H} originates from the fact that in

environments with multipath impairment, the transmitted signal is scattered into many paths and grouped into clusters. Paths of each cluster have relatively the same time delay and therefore cannot be distinguished by the receiver, where each cluster has non resolvable paths in time domain. Consequently, rank order is determined by the number of clusters that have significant power. As an example, suppose that the signal is reflected from three scatters into three resolvable clusters. If two of them own a high percentage of signal power, then rank-two order is existed and so on. The rank analysis of \mathbf{H} and rank order selection are accomplished by adopting SVD and truncated SVD techniques [7, 8]. Reduced rank channel is used to construct a new set of JCE and MUJD algorithms. Unlike previous multi-cell works, the analysis in this paper involves extending model that consider that all the K users in the serving cell are active in addition to some of interfering users.

The simulation results have been shown the validity of the extension of multi-cell joint channel estimation method over the conventional methods. Also, the reduced rank technique enhances the Multi-cell model with efficient way to reduce the complexity that result from the new algorithm by the estimation process for the interferer users. Simulation results showed that multi-cell reduced rank channel estimators and their data detectors have better performance than traditional full rank multi user estimators and detectors. Our simulations tested the proposed estimator under worst interference situation ($SIR = -12$ dB), were done at two scenarios of users' movements, 3 and 120 km/h (indoor B and vehicular A channels) according to international telecommunication union (ITU) standard. In all of these cases, the proposed technique has the superior performance over the traditional of single-cell and multi-cell estimators.

The rest of the paper is organized as follows. The system model for TD-SCDMA is presented in Sect. 2. Joint channel estimation for serving and multi-cell are developed in Sect. 3. In Sect. 4, the reduced rank channel estimation is modeled and analyzed. The common MUJD detectors used in TD-SCDMA system ZF-BLE and MMSE-BLE are introduced and discussed in Sect. 5. Section 6, presents the simulation results describes in the system performance under the proposed algorithms. The conclusions are summarized in Sect. 7.

2 System model

2.1 Background

The physical channels in TD-SCDMA system are defined in terms of frequency, time, and code. Both uplink and downlink channels have the same carrier frequency; however, Time Division Duplexing (TDD) is used for

distinguishing between them. In general, the time dimension of the physical channels is divided by the Time Division Multiple Access (TDMA) scheme into a three-layer structure. For specific illustration, the $(1/T_c) = 1.28$ Mcps option of TD-SCDMA systems will be considered throughout this paper, where T_c is the chip period. The first layer is called the radio frame of 10 ms duration and is divided by the second layer into two subframes of 5 ms and 6,400 chips each. The third layer has seven traffic Time Slots (TS) of 864 chips (675 μ s duration) each, a downlink time slot of 96 chips (75 μ s), an uplink pilot time slot of 160 chips (125 μ s), and a main guard period of 96 chips (75 μ s) for TDD operation. The first slot in the subframe, i.e., TS0, is assigned only for downlink, while TS1 is always allocated for uplink, and the remaining traffic slots might be assigned to the uplink or the downlink [9].

The physical content of the traffic time slot is called the burst, which has the same length as the slot. The burst is organized as follows: two data blocks of 352 chips each, a midamble (training sequence) of $L = 144$ chips, and a Guard Period (GP) of 16 chips, as shown in Fig. 1. The system offers the transmission of a maximum of $K_{max} = 16$ users during one time slot. The burst of each user is distinguished from other users by scrambling its data with a specific signature code and laying a certain midamble. The total resulted time-coded slot is oversampled and shaped using Root Raised Cosine (RRC) filter with roll-off factor of (0.22) [10]. The complete block diagram of the transmitting and receiving parts as well as the channel of the TD-SCDMA system is shown in Fig. 2.

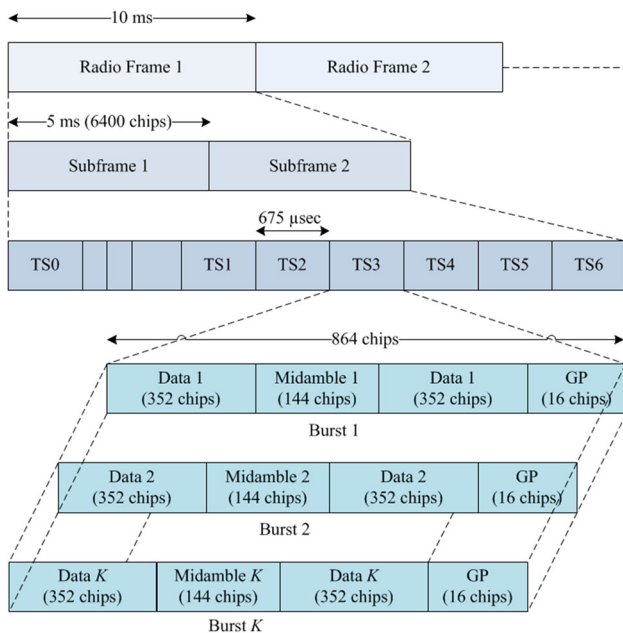


Fig. 1 Radio frame, subframe, and time slot physical structure frame

In general, there are 128 available basic code midambles; however each cell is restricted to use only four codes. The base station selects one of the four codes and assigns it, after some modifications, to the active users. The real valued basis midamble code vector \mathbf{u} is defined as [11],

$$\mathbf{u} = [u(1) \ \cdots \ u(p) \ \cdots \ u(P)] \tag{1}$$

where $u(p) \in \{1, -1\}$, indicates the elements of the \mathbf{u} vector; and $P = K \times W = 128$ where the parameter P relates between the channel delay length W that is measured in chips and the planned K users in serving cell [11]. The extended periodic training sequence vector \mathbf{m} is define as,

$$\mathbf{m} = [m(1) \ m(2) \ \cdots \ m(L + (K - 1)W)] \tag{2}$$

where the elements $m(i)$ of the vector \mathbf{m} are obtained from \mathbf{u} according to:

$$m(i) = \begin{cases} u(i), & \text{for } i = 1, \dots, P \\ u(i - P), & \text{for } i = P + 1, \dots, L + (K - 1)W \end{cases} \tag{3}$$

Accordingly, the complex valued training sequence elements $m_k(i)$ for the k th user are calculated from $m(i)$ as follow:

$$m_k(i) = (j)^i m(i + (K - k)W), \tag{4}$$

for $i = 1, \dots, L$ and $k = 1, \dots, K$

Thus, the midamble of each user is a cyclically shifted version of \mathbf{m} .

2.2 Serving-cell midamble model

Suppose the uplink transmission is done over a multipath Rayleigh faded channel with ambient Gaussian distributed noise of zero mean and variance σ^2 . In serving cell midamble model, inter-cell interference is ignored by the receiver and considered as noise. The received signal corresponding to the transmitted complex midambles of the different users located in the same serving cell is,

$$\begin{aligned} \mathbf{r}_m &= \sum_{k=1}^K [m_k(1) \cdots m_k(i) \cdots m_k(L)] * \begin{bmatrix} h_k(1) \\ \vdots \\ h_k(w) \\ \vdots \\ h_k(W) \end{bmatrix} + \begin{bmatrix} n_1 \\ \vdots \\ n_p \\ \vdots \\ n_P \end{bmatrix} \\ &= \sum_{k=1}^K \mathbf{m}_k * \mathbf{h}_k + \mathbf{n}_m \end{aligned} \tag{5}$$

where, \mathbf{r}_m is a $P \times 1$ received midambles vector depicted in (6); \mathbf{m}_k is a $1 \times L$ midamble vector of the k th user with its elements as defined in (4); \mathbf{h}_k is a $W \times 1$ CIR vector for the

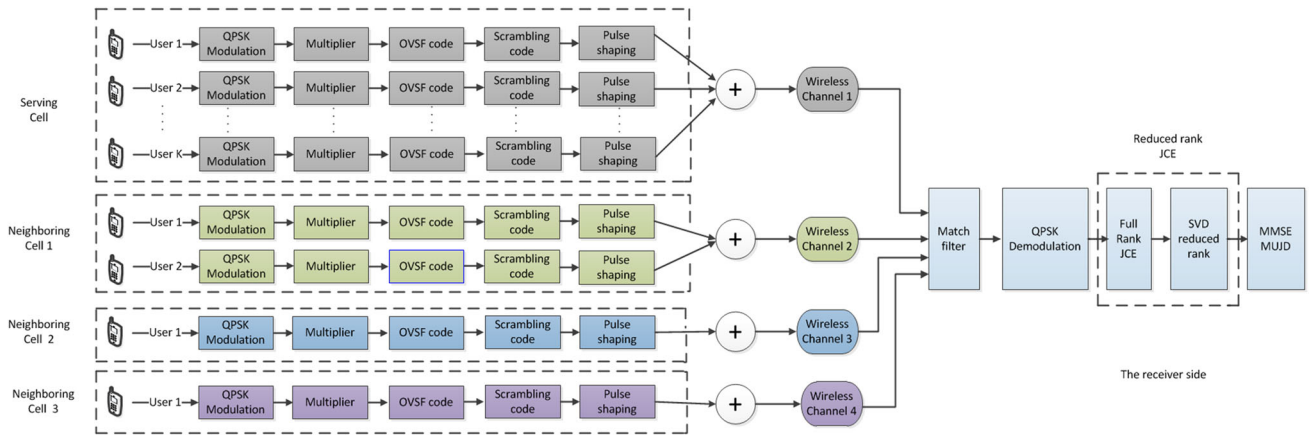


Fig. 2 Block diagram of the transmitter and receiver parts of multiplier

k th user such that it accounts for transmitter filter, propagation channel, and receiver filter; (*) denotes the notation of convolution operation; and \mathbf{n}_m is a $P \times 1$ noise vector. Equation (5) justifies the appearance of ISI in TD-SCDMA system since each present chip depends on $W - 1$ previous chips. Thus, the first $W - 1$ samples of the received vector \mathbf{r}_m in (5) are discarded to exclude the received vector from data dependency. The noise term of (5) includes additive white noise and inter-cell interference.

The received midamble vector is described as:

$$\mathbf{r}_m = [r(W) \quad r(W + 1) \quad \dots \quad r(P + W - 1)]^T \tag{6}$$

the K midambles and CIR vectors of (5) can be collected into a single matrix and single vector, respectively, as:

$$\begin{aligned} \mathbf{r}_m &= \sum_{k=1}^K \mathbf{G}_k \mathbf{h}_k + \mathbf{n}_m = [\mathbf{G}_1 \quad \mathbf{G}_2 \quad \dots \quad \mathbf{G}_K] \begin{bmatrix} \mathbf{h}_1 \\ \mathbf{h}_2 \\ \vdots \\ \mathbf{h}_K \end{bmatrix} + \mathbf{n}_m \\ &= \mathbf{G}_{sc} \mathbf{h}_{sc} + \mathbf{n}_m \end{aligned} \tag{7}$$

where, \mathbf{G}_k is the $P \times W$ Toeplitz midamble matrix defined in (8) such that it transforms the convolution of (5) into a multiplication; \mathbf{G}_{sc} is the $P \times P$ square cyclic matrix that collects \mathbf{G}_k for all the K users in the same serving cell; and \mathbf{h}_{sc} is the $P \times P$ channel impulse vector for the K users in the serving cell only.

$$\mathbf{G}_k = \begin{bmatrix} m_k(W) & m_k(W - 1) & \dots & m_k(1) \\ m_k(W + 1) & m_k(W) & \dots & m_k(2) \\ \vdots & \vdots & \ddots & \vdots \\ m_k(P + W - 1) & m_k(P + W - 2) & \dots & m_k(P) \end{bmatrix} \tag{8}$$

It is seen that the cyclic feature of the matrix \mathbf{G}_{sc} is very useful in the simplification of channel computation,

which will be discussed in Sect. 3. The cyclicity of a matrix indicates that each column is generated from the left on by rotating it, and the sum of each row and column is the same. Equation (9) describes an arbitrary cyclic matrix \mathbf{C} .

$$\mathbf{C} = \begin{bmatrix} c_1 & c_4 & c_3 & c_2 \\ c_2 & c_1 & c_4 & c_3 \\ c_3 & c_2 & c_1 & c_4 \\ c_4 & c_3 & c_2 & c_1 \end{bmatrix} \tag{9}$$

2.3 Multi-cell midamble model

Suppose the interfering users from other adjacent cells have significant power comparable to the users of the serving cell. In this paper, the multi-cell midamble model will be developed according to the following two cases.

- *Case 1* Suppose the number of active users in the serving cell is $K_1 < K$. Also, suppose the number of interfering users with strong power from adjacent cells is $K_2 < K$. The $1 \times L$ midamble sequence vector and $W \times 1$ CIR of interfering users are denoted as \mathbf{m}'_k and \mathbf{h}'_k , respectively, for $k = 1, \dots, K_2$. The received signal of (5) might be reformed to include the interfering users as,

$$\mathbf{r}_m = \sum_{k=1}^{K_1} \mathbf{m}_k * \mathbf{h}_k + \sum_{k=1}^{K_2} \sqrt{J_k} \mathbf{m}'_k * \mathbf{h}'_k + \mathbf{n}_m \tag{10}$$

where, $\sqrt{J_k}$ is the power of the inter-cell interfering users for $k = 1, \dots, K_2$, and the power of the active users within the serving cell is considered to be unity. The noise is Additive White Gaussian Noise (AWGN) with zero and variance σ^2 . The $P \times W$ convolution midamble matrix of the interfering users is defined as \mathbf{G}'_k for $k = 1, \dots, K_2$, and then (10) is rewritten as:

$$\mathbf{r}_m = \sum_{k=1}^{K_1} \mathbf{G}_k \mathbf{h}_k + \sum_{k=1}^{K_2} \sqrt{J_k} \mathbf{G}'_k \mathbf{h}'_k + \mathbf{n}_m$$

$$= \begin{bmatrix} \mathbf{G}_1 & \cdots & \mathbf{G}_{K_1} & \sqrt{J_1} \mathbf{G}'_1 & \cdots & \sqrt{J_{K_2}} \mathbf{G}'_{K_2} \end{bmatrix} \begin{bmatrix} \mathbf{h}_1 \\ \vdots \\ \mathbf{h}_{K_1} \\ \mathbf{h}'_1 \\ \vdots \\ \mathbf{h}'_{K_2} \end{bmatrix} + \mathbf{n}_m$$

$$= \mathbf{G}_{mc} \mathbf{h}_{mc} + \mathbf{n}_m \tag{11}$$

where, \mathbf{G}_{mc} is the $P \times (K_1 + K_2)$ multi-cell midamble matrix for K_1 active users in the serving cell and K_2 significant interfering users from neighboring cells and \mathbf{h}_{mc} is the $(K_1 + K_2)W \times 1$ CIR vector for all the active and interfering users. It should be noted that \mathbf{G}_{mc} is no longer cyclic as each adjacent cell has its own basis midamble code \mathbf{u} different from that of the serving cell. \mathbf{G}_{mc} is non square and can be made square matrix if the following condition is verified: $K = K_1 + K_2$. In these circumstances, the serving cell cyclic midamble matrix \mathbf{G}_{sc} and native CIR \mathbf{h}_{sc} of (7) are completely replaced by the non cyclic multi-cell midamble matrix \mathbf{G}_{mc} and hybrid CIR \mathbf{h}_{mc} , respectively.

- *Case 2* If all users within the serving cell are active, i.e., $K_1 = K$, associated with K_2 strong interferes from adjacent cells, the new set of equations of the received midamble will be,

$$\mathbf{r}_m = \sum_{k=1}^K \mathbf{m}_k * \mathbf{h}_k + \sum_{k=1}^{K_2} \sqrt{J_k} \mathbf{m}'_k * \mathbf{h}'_k + \mathbf{n}_m$$

$$\mathbf{r}_m = \sum_{k=1}^K \mathbf{G}_k \mathbf{h}_k + \sum_{k=1}^{K_2} \sqrt{J_k} \mathbf{G}'_k \mathbf{h}'_k + \mathbf{n}_m$$

$$= \begin{bmatrix} \mathbf{G}_1 & \cdots & \mathbf{G}_K & \sqrt{J_1} \mathbf{G}'_1 & \cdots & \sqrt{J_{K_2}} \mathbf{G}'_{K_2} \end{bmatrix} \begin{bmatrix} \mathbf{h}_1 \\ \vdots \\ \mathbf{h}_K \\ \mathbf{h}'_1 \\ \vdots \\ \mathbf{h}'_{K_2} \end{bmatrix} + \mathbf{n}_m$$

$$= \mathbf{G}'_{mc} \mathbf{h}'_{mc} + \mathbf{n}_m \tag{12}$$

where \mathbf{G}'_{mc} is the $P \times (K + K_2)W$ non cyclic non square multi-cell midamble matrix for users from serving cell and adjacent cells and \mathbf{h}'_{mc} is the $(K + K_2)W \times 1$ CIR vector for all the intended users.

2.4 Data model

It is convenient to take one block of data at a time (before the midamble) to formulate a data system model when users of the serving cell transmit data symbols. The k th user transmits N_k QPSK modulated data symbols during the time slot arranged in the vector below:

$$\mathbf{d}_k = [d_k(1) \cdots d_k(i) \cdots d_k(N_k)]^T, \quad k = 1, \dots, K \tag{13}$$

where, each symbol value $\in \{1, j, -1, -j\}$. For the k th user, each modulated data symbol is spread using a channelization code Q_k for $k = 1, \dots, K$ of a variable length $\in \{1, 2, 4, 8, 16\}$. The channelization codes are generated using Orthogonal Variable Spreading Factor (OVSF) codes. The number of data symbols N_k of the user in each block and symbol duration $T_{s,k}$ depend on the spreading factor such that $N_k = (352/Q_k)$ and $T_{s,k} = Q_k T_c$, respectively.

Subsequently, the spread symbol of each user is multiplied by a code-specific multiplier and scrambled by a cell-specific complex code having a length of 16 [10]. Further, the combination of the user specific channelization code with multiplier and cell specific scrambling code is defined as a user and cell specific spreading code,

$$\mathbf{s}_k = [s_k(1) s_k(2) \cdots s_k(Q_k)]^T, \quad k = 1, \dots, K \tag{14}$$

The outcome of the scrambling process to the data vector can be expressed in terms of Kronecker production as,

$$\mathbf{s}_k \otimes \mathbf{d}_k = \begin{bmatrix} \mathbf{s}_k & 0 & 0 & 0 \\ 0 & \mathbf{s}_k & 0 & 0 \\ 0 & 0 & \ddots & 0 \\ 0 & 0 & 0 & \mathbf{s}_k \end{bmatrix} \mathbf{d}_k = \mathbf{S}_k \mathbf{d}_k \tag{15}$$

where, \otimes is the Kronecker operator symbol and \mathbf{S}_k is a $NQ \times N$ diagonal scrambling matrix for the k th user. The received signal corresponding to the transmitted data of the K users is,

$$\mathbf{r}_d = \sum_{k=1}^K \mathbf{h}_k * \mathbf{s}_k \otimes \mathbf{d}_k + \mathbf{n}_d \tag{16}$$

where, \mathbf{r}_d is a $(NQ + W - 1) \times 1$ vector defined in (16) that accounts for the received symbols corresponding to the transmitted chips and \mathbf{n}_d is a $(NQ + W - 1) \times 1$ ambient noise and inter-cell interference vector.

$$\mathbf{r}_d = [r(1) \quad r(2) \quad \cdots \quad r(NQ + W - 1)]^T \tag{17}$$

Further, if the convolution of channel impulse response and scrambling code in (16) is combined into a single vector of $(Q + W - 1) \times 1$ dimension as shown below,

$$\mathbf{b}_k = [b_k(1) \cdots b_k(Q + W - 1)]^T \tag{18}$$

and if (15) is substituted in (16), then, \mathbf{r}_d can be re-written in a more compact form:

$$\begin{aligned} \mathbf{r}_d &= \sum_{k=1}^K \underbrace{\begin{bmatrix} \mathbf{b}_{k_1} & \dots & \mathbf{0} \\ \vdots & & \vdots \\ \mathbf{0} & \dots & \mathbf{b}_{k_K} \end{bmatrix}}_N \mathbf{d}_k + \mathbf{n}_d \\ &= \sum_{k=1}^K \mathbf{A}_k \mathbf{d}_k + \mathbf{n}_d = [\mathbf{A}_1 \dots \mathbf{A}_K] \cdot \begin{bmatrix} \mathbf{d}_1 \\ \vdots \\ \mathbf{d}_K \end{bmatrix} + \mathbf{n}_d \\ &= \mathbf{A}_{sc} \mathbf{d}_{sc} + \mathbf{n}_d \end{aligned} \tag{19}$$

where, \mathbf{A}_k is a $(NQ + W - 1) \times N$ block Toeplitz system matrix that combines the effect of CIR and scrambling code for the k th user, \mathbf{A}_{sc} is a $(NQ + W - 1) \times NK$ banded Toeplitz matrix that collects the system matrices of the K users into a single one, and \mathbf{d}_{sc} is a $(NK) \times 1$ data vector for all the K users in the serving cell only.

For a multi-cell situation with case 1, this data model can be obtained in a straightforward manner from a single cell case. Define \mathbf{d}'_k , \mathbf{s}'_k , \mathbf{b}'_k and \mathbf{A}'_k as the $N \times 1$ data vector, $Q \times 1$ spreading code vector, $(Q + W - 1) \times 1$ combined CIR and $(NQ + W - 1) \times N$ block Toeplitz matrix of the interfering users, respectively, for $k = 1, \dots, K_2$. Thus, the multi-cell data model is,

$$\begin{aligned} \mathbf{r}_d &= \sum_{k=1}^{K_1} \mathbf{A}_k \mathbf{d}_k + \sum_{k=1}^{K_2} \sqrt{J_k} \mathbf{A}'_k \mathbf{d}'_k + \mathbf{n}_d \\ &= [\mathbf{A}_1 \dots \mathbf{A}_{K_1} \sqrt{J_1} \mathbf{A}'_1 \dots \sqrt{J_{K_2}} \mathbf{A}'_{K_2}] \cdot \begin{bmatrix} \mathbf{d}_1 \\ \vdots \\ \mathbf{d}_{K_1} \\ \mathbf{d}'_1 \\ \vdots \\ \mathbf{d}'_{K_2} \end{bmatrix} + \mathbf{n}_d \\ &= \mathbf{A}_{mc} \mathbf{d}_{mc} + \mathbf{n}_d \end{aligned} \tag{20}$$

where, \mathbf{A}_{mc} is the $(NQ + W - 1) \times N(K_1 + K_2)$ multi-cell banded Toeplitz matrix that combines all the matrices of desired and interfering users, \mathbf{d}_{mc} is a $N(K_1 + K_2) \times 1$

total data vector, and \mathbf{n}_d is the ambient noise alone. When $K_1 + K_2 = K$, the serving cell data model is fully exchanged by the multi-cell model.

Similarly, for case 2 of the multi-cell model, the new equations are,

$$\begin{aligned} \mathbf{r}_d &= \sum_{k=1}^{K_1} \mathbf{A}_k \mathbf{d}_k + \sum_{k=1}^{K_2} \sqrt{J_k} \mathbf{A}'_k \mathbf{d}'_k + \mathbf{n}_d \\ &= [\mathbf{A}_1 \dots \mathbf{A}_K \sqrt{J_1} \mathbf{A}'_1 \dots \sqrt{J_{K_2}} \mathbf{A}'_{K_2}] \cdot \begin{bmatrix} \mathbf{d}_1 \\ \vdots \\ \mathbf{d}_K \\ \mathbf{d}'_1 \\ \vdots \\ \mathbf{d}'_{K_2} \end{bmatrix} + \mathbf{n}_d \\ &= \mathbf{A}'_{mc} \mathbf{d}'_{mc} + \mathbf{n}_d \end{aligned} \tag{21}$$

where, \mathbf{A}'_{mc} is a $(NQ + W - 1) \times N(K + K_2)$ multi-cell banded Toeplitz matrix for the active and interfering users and \mathbf{d}'_{mc} is a $N(K + K_2) \times 1$ total data vector.

3 Joint channel estimation (JCE)

3.1 Serving-cell channel estimation

Practically, spreading codes allocated for a specified cellular cell are not fully orthogonal especially in multipath environments; this makes MAI effectively obvious in a single user detection fashion. Therefore, multi-user joint detection is preferred in TD-SCDMA systems. As will be explained in Sect. 5, the joint data detection is based on providing a proper estimated channel. An estimation version of the total channel impulse response for all users could be obtained by using the least square optimization criterion on (7). The serving cell least square CIR estimation, $\hat{\mathbf{h}}_{LS-sc}$, is given by [12],

$$\hat{\mathbf{h}}_{LS-sc} = (\mathbf{G}_{sc}^H \mathbf{G}_{sc})^{-1} \mathbf{G}_{sc}^H \mathbf{r}_m \tag{22}$$

where $(\cdot)^H$ denotes the Hermitian transpose and the channel is assumed to be an FIR filter. As the matrix \mathbf{G}_{sc} is cyclic, the LS channel estimation reduces to the Steiner estimator,

$$\hat{\mathbf{h}}_{LS-sc} = \mathbf{G}_{sc}^{-1} \mathbf{r}_m \tag{23}$$

the computation demand for \mathbf{G}_{sc}^{-1} is facilitated using Fast Fourier Transform (FFT) and Inverse Fast Fourier Transform (IFFT) [13]. For complete analysis, (7) is substituted in (23) to express the amount of error implied in LS solution,

$$\hat{\mathbf{h}}_{LS-sc} = \mathbf{h}_{sc} + \mathbf{G}_{sc}^{-1} \mathbf{n}_m \tag{24}$$

The last result reveals that the LS estimated channel deviates from the actual value by $\mathbf{G}_{sc}^{-1} \mathbf{n}_m$ in the presence of ambient noise. The smallest noise term of (24), the closest LS estimated CIR from the actual one. That is, if the serving cell midamble matrix \mathbf{G}_{sc} is singular or near it, the noise term $\mathbf{G}_{sc}^{-1} \mathbf{n}_m$ is tremendously amplified, thereby causing a greater error in channel estimation.

To overcome the drawback of the LS method, the MMSE optimization criterion provides better behavior against noise. The estimated MMSE CIR, $\hat{\mathbf{h}}_{MMSE-sc}$, is [11],

$$\hat{\mathbf{h}}_{MMSE-sc} = (\mathbf{G}_{sc}^H \mathbf{G}_{sc} + \sigma^2 \mathbf{R}_h)^{-1} \mathbf{G}_{sc}^H \mathbf{r}_m \tag{25}$$

where $\mathbf{R}_h = E\{\mathbf{h}_{sc} \mathbf{h}_{sc}^H\}$ is the $P \times P$ correlation matrix of the total CIR \mathbf{h}_{sc} as described in (26), where, $E\{\cdot\}$ is the expectation or mean operator.

$$\mathbf{R}_h = \begin{bmatrix} E\{\mathbf{h}_1 \mathbf{h}_1^H\} & E\{\mathbf{h}_1 \mathbf{h}_2^H\} & \cdots & E\{\mathbf{h}_1 \mathbf{h}_K^H\} \\ E\{\mathbf{h}_2 \mathbf{h}_1^H\} & E\{\mathbf{h}_2 \mathbf{h}_2^H\} & \cdots & E\{\mathbf{h}_2 \mathbf{h}_K^H\} \\ \vdots & \vdots & \ddots & \vdots \\ E\{\mathbf{h}_K \mathbf{h}_1^H\} & E\{\mathbf{h}_K \mathbf{h}_2^H\} & \cdots & E\{\mathbf{h}_K \mathbf{h}_K^H\} \end{bmatrix} \tag{26}$$

If the users’ channels are independent of each other, i.e., $E\{\mathbf{h}_i \mathbf{h}_j^H\} = 0$, and have unity gains, that is, $E\{|\mathbf{h}_k|^2\} = 1$, then (26) becomes,

$$\hat{\mathbf{h}}_{MMSE-sc} = (\mathbf{G}_{sc}^H \mathbf{G}_{sc} + \sigma^2 \mathbf{I})^{-1} \mathbf{G}_{sc}^H \mathbf{r}_m \tag{27}$$

where, \mathbf{I} is the identity matrix of $P \times P$ dimension. The error in MMSE solution can be expressed as (7) and is substituted in (27),

$$\begin{aligned} \hat{\mathbf{h}}_{MMSE-sc} &= (\mathbf{G}_{sc}^H \mathbf{G}_{sc} + \sigma^2 \mathbf{I})^{-1} \mathbf{G}_{sc}^H \times (\mathbf{G}_{sc} \mathbf{h}_{sc} + \mathbf{n}_m) \\ &= (1 + \sigma^2 \mathbf{I} (\mathbf{G}_{sc}^H \mathbf{G}_{sc})^{-1})^{-1} \mathbf{h}_{sc} \\ &\quad + (1 + \sigma^2 \mathbf{I} (\mathbf{G}_{sc}^H \mathbf{G}_{sc})^{-1})^{-1} \mathbf{G}_{sc}^{-1} \mathbf{n}_m \end{aligned} \tag{28}$$

where the first term of (28) represents the actual CIR plus a contribution from residual MAI owing to the lack of orthogonal midamble codes and the second term accounts for noise. The MMSE estimator can achieve the LS solution as the noise variance approaches zero.

3.2 Multi-cell channel estimation

In the presence of strong power inter-cell interference, the SC-JCE algorithms would suffer from a significant degradation in performance and the prescribed LS and MMSE solutions would be biased by the variance of inter-cell interference. Thus, multi-cell JCE is a suitable option to overcome this problem. The optimization criteria applied in advance for serving cell estimation section could be

extended in a straight forward manner to determine the estimated CIR of users belonging to the serving and interfering cells together. However, the lack of cyclic property of the Toeplitz midamble matrices \mathbf{G}_{mc} and \mathbf{G}'_{mc} prevents the application of the Steiner algorithm and the exploitation of the FFT and IFFT facilities. Moreover, blind identification is required for estimating the midamble sequence of each interfering user [14].

Similarity between the serving cell and multi-cell midambles models in the developed equations, makes the multi-cell LS based joint CIR estimation easily expandable from (22) as,

$$\hat{\mathbf{h}}_{LS-mc} = (\mathbf{G}_{mc}^H \mathbf{G}_{mc})^{-1} \mathbf{G}_{mc}^H \mathbf{r}_m \tag{29a}$$

$$\hat{\mathbf{h}}'_{LS-mc} = (\mathbf{G}'_{mc}{}^H \mathbf{G}'_{mc})^{-1} \mathbf{G}'_{mc}{}^H \mathbf{r}_m \tag{29b}$$

where $\hat{\mathbf{h}}_{LS-mc}$ and $\hat{\mathbf{h}}'_{LS-mc}$ represent the multi-cell estimated CIR for cases one and two of $K_1 + K_2$ and $K + K_2$ intended users, respectively. Errors in multi-cell LS estimators become $(\mathbf{G}_{mc}^H \mathbf{G}_{mc})^{-1} \mathbf{G}_{mc}^H \mathbf{n}_m$ and $(\mathbf{G}'_{mc}{}^H \mathbf{G}'_{mc})^{-1} \mathbf{G}'_{mc}{}^H \mathbf{n}_m$ for cases one and two, respectively.

Multi-cell joint MMSE estimators are directly captured from (27) as,

$$\hat{\mathbf{h}}_{MMSE-mc} = (\mathbf{G}_{mc}^H \mathbf{G}_{mc} + \sigma^2 \mathbf{I})^{-1} \mathbf{G}_{mc}^H \mathbf{r}_m \tag{30a}$$

$$\hat{\mathbf{h}}'_{MMSE-mc} = (\mathbf{G}'_{mc}{}^H \mathbf{G}'_{mc} + \sigma^2 \mathbf{I})^{-1} \mathbf{G}'_{mc}{}^H \mathbf{r}_m \tag{30b}$$

where $\hat{\mathbf{h}}_{MMSE-mc}$ and $\hat{\mathbf{h}}'_{MMSE-mc}$ represent the multi-cell estimated CIR for cases one and two, respectively. Errors in Multi-cell MMSE estimators are a direct extension of (28). Contrary to SC-JCE, MC-JCE solutions are unbiased estimators.

3.3 Post processing

In general, few taps of the estimated CIR according to LS and MMSE methods represent multipath and the remaining are from noise. Therefore, an improvement is made by comparing the channel taps of each user against a noise threshold value such that [14],

$$\hat{h}_k(w) = \begin{cases} \hat{h}_k(w) & \text{if } \|\hat{h}_k(w)\|^2 \geq c \times \sigma^2 \\ 0 & \text{if } \|\hat{h}_k(w)\|^2 < c \times \sigma^2 \end{cases} \tag{31}$$

where $\hat{h}_k(w)$ is the estimated w th tap’s value of the k th user, c is a constant with empirical value, and $\|\hat{h}_k(w)\|^2$ is the tap’s power. Such post processing mechanism directly follows SC-JCE and MC-JCE algorithms, where a comparison is made between the value of tap’s power with the variance of the noise to decide whether the tap exists or not. In [8], a modification post processing method is adopted for the criterion mentioned in (31) to improve the channel estimation.

4 Reduced rank channel estimation

4.1 Problem formulation

As will be shown in Sect. 5, the performance of data detection algorithms depends mainly on the accuracy of CIR fed by the channel estimators. The channels of uplink users require the estimation of $K \times W = 128$ parameters in the serving cell model during a block of training chips equal to $P = 128$. Without any doubt, it is not correct to hold such an estimation process that might lead to several unavoidable negatives, the most important being that estimation has a high variance from the actual solution. This is owing to the high number of estimated parameters corresponding to the availability of short training sequences in TD-SCDMA systems. Secondly, the large number of parameters to be estimated will complicate algorithms for estimation; which will make them more time consuming to execute. Finally, in fast varying environments the channel cannot be made adaptive on a symbol-by-symbol basis with such a large number of parameters required. In the multi-cell model, the situation is worse than in the serving cell, especially in the second case where the number of unknown parameters is $(K + K_2) \times W > 128$. For numerical example, consider $K = 8$, $K_2 = 4$, and $W = 16$, then the number of required parameters is 192 that must be estimated during 128 chips, or in other words, there is a need to calculate and eventually implement one and a half parameters per one chip period.

The key solution to the chain of problems mentioned above is to reduce the number of unknowns to simplify their estimation. This reduction is possible if the constructed matrix of the total temporal channel in TD-SCDMA systems is rank deficient, which means that there is a correlation among its elements. The basis of this possibility in multipath environments with single antenna occurs when the delay spread is lower than the symbol period of the communication system.

4.2 Reduced rank model

In environments with multipath impairment, the transmitted signal is scattered into several paths and grouped into clusters. Paths of each cluster have relatively the same time delay and therefore cannot be distinguished by the receiver. In order to modalize the reduced rank model for the joint CIR in TD-SCDMA systems, the following transformations are introduced:

$$\begin{aligned} & \text{matrix}([a_1 \ \cdots \ a_W \ a_{W+1} \ \cdots \ a_{2W}]^T) \\ &= \begin{bmatrix} a_1 & \cdots & a_W \\ a_{W+1} & \cdots & a_{2W} \end{bmatrix} \end{aligned} \quad (32)$$

where matrix (\cdot) is the operator that transforms the column vector to a matrix by stacking a block of W elements into a row. For a generalized framework, a total CIR is defined that collects M CIRs such that $M < W$ and (32) is applied as,

$$\begin{aligned} \mathbf{H} &= \text{matrix} \left(\begin{bmatrix} \mathbf{h}_1 \\ \vdots \\ \mathbf{h}_m \\ \vdots \\ \mathbf{h}_M \end{bmatrix} \right) \\ &= \begin{bmatrix} h_{1,1} & \cdots & h_{1,w} & \cdots & h_{1,W} \\ \vdots & & & & \vdots \\ h_{m,1} & & \ddots & & h_{m,W} \\ \vdots & & & & \vdots \\ h_{M,1} & \cdots & h_{M,w} & \cdots & h_{M,W} \end{bmatrix} \end{aligned} \quad (33)$$

where \mathbf{H} is the $M \times W$ channel matrix with a rank order of $\min(M, W) = M$. The SVD algorithm will be used as an analytical tool for investigating the structural content of the constructed channel matrix \mathbf{H} :

$$\mathbf{H} = \mathbf{U}\mathbf{\Gamma}\mathbf{V}^H = \sum_{i=1}^{r_o} \mathbf{u}_i \lambda_i \mathbf{v}_i^H, \quad r \leq M \quad (34)$$

where r_o is the largest rank order of the full rank channel matrix \mathbf{H} , $\mathbf{\Gamma} = \text{diag}(\lambda_1 \ \cdots \ \lambda_{r_o})$ is the $r_o \times r_o$ diagonal matrix of the singular values arranged in non-increasing order, $\lambda_1 \geq \lambda_2 \geq \cdots \geq \lambda_{r_o}$; and $\mathbf{U} = [\mathbf{u}_1 \ \cdots \ \mathbf{u}_{r_o}]$ and $\mathbf{V} = [\mathbf{v}_1 \ \cdots \ \mathbf{v}_{r_o}]$ are unitary matrices that denote the $M \times r_o$ and $r_o \times W$ right singular vectors corresponding to the largest singular values, respectively. The full rank \mathbf{H} could be approximated to a reduced rank matrix \mathbf{H}_r by selecting a rank order value r lower than r_o . Thus,

$$\mathbf{H}_r = \mathbf{U}_r \mathbf{\Gamma}_r \mathbf{V}_r^H = \sum_{i=1}^r \mathbf{u}_i \lambda_i \mathbf{v}_i^H, \quad r \leq r_o \quad (35)$$

where \mathbf{H}_r is the reduced rank channel matrix formed from truncated SVD, $\mathbf{\Gamma}_r = \text{diag}(\lambda_1 \ \cdots \ \lambda_r)$, $\mathbf{U}_r = [\mathbf{u}_1 \ \cdots \ \mathbf{u}_r]$, and $\mathbf{V}_r = [\mathbf{v}_1 \ \cdots \ \mathbf{v}_r]$ SVD divides the space of the channel matrix into two subspaces, the first r columns assigned for signal subspace and the remaining $r_o - r$ for noise subspace. Hence, matrix \mathbf{H}_r has a total of $r(M + W)$ essential parameters that is lower than the unreduced channel matrix MW .

4.3 Analysis and performance

The performance of the different estimator is a function of channel estimation accuracy. The comparison among them can be evaluated by two aspects. The first one is the normalised mean square error (MSE); the second one is the correlation coefficient.

4.3.1 The normalized MSE

The normalised MSE is calculated by averaging complex magnitude error between the ideal CIR and the estimated CIR. Thus, using the operator of (32), CIR vector \mathbf{h}_{sc} results in \mathbf{H}_{sc} , the channel matrix of KW dimensions for the serving cell. The performance of the reduced rank channel and the validity of the rank order are evaluated in term of the normalized MSE as follow:

$$\text{MSE} = \frac{\|\mathbf{H}_r - \mathbf{H}\|^2}{\|\mathbf{H}\|^2} = \frac{\sum_{i=r+1}^{r_o} \lambda_i^2}{\sum_{i=1}^{r_o} \lambda_i^2} \tag{36}$$

where \mathbf{H} is the actual channel matrix. In simulations, normalised MSE is used for determining the effective rank order in the TD-SCDMA system according to the defined physical channels.

4.3.2 The correlation coefficient

The correlation coefficient measures the linear strength relationship between the ideal CIR and the estimated CIR. Equivalent data sets converge to a correlation coefficient equal to one, while uncorrelated data result in a zero value for the correlation coefficient. The correlation coefficient of the channel matrix is defined as

$$C.C = \frac{\sum_i \sum_j (\mathbf{H}_{ij} - \bar{\mathbf{H}})(\hat{\mathbf{H}}_{ij} - \hat{\mathbf{H}})}{\sqrt{(\sum_i \sum_j (\mathbf{H}_{ij} - \bar{\mathbf{H}})^2)(\sum_i \sum_j (\hat{\mathbf{H}}_{ij} - \hat{\mathbf{H}})^2)}} \tag{37}$$

where \mathbf{H}_{ij} is the actual channel matrix, $\bar{\mathbf{H}}$ is the mean of the actual channel matrix elements, $\hat{\mathbf{H}}_{ij}$ is the channel matrix estimated by reduced rank estimator, and $\hat{\mathbf{H}}$ is the mean of the channel matrix elements estimated by reduced rank estimator.

5 Multi user joint detection (MUJD)

For data detection, the MUJD methods have shown superior performance when compared to single user detection. Among the joint detection methods, two well known linear equalizers are presented in this paper, namely, the ZF-BLE and MMSE-BLE joint detectors, respectively. Recovered data according to ZF-BLE, for single cell and multi-cell users are given by [13],

$$\hat{\mathbf{d}}_{ZF-sc} = (\mathbf{A}_{sc}^H \mathbf{R}_n^{-1} \mathbf{A}_{sc})^{-1} \mathbf{A}_{sc}^H \mathbf{R}_n^{-1} \mathbf{r}_d \tag{38a}$$

$$\hat{\mathbf{d}}_{ZF-mc} = (\mathbf{A}_{mc}^H \mathbf{R}_n^{-1} \mathbf{A}_{mc})^{-1} \mathbf{A}_{mc}^H \mathbf{R}_n^{-1} \mathbf{r}_d \tag{38b}$$

$$\hat{\mathbf{d}}'_{ZF-mc} = (\mathbf{A}'_{mc}{}^H \mathbf{R}_n^{-1} \mathbf{A}'_{mc})^{-1} \mathbf{A}'_{mc}{}^H \mathbf{R}_n^{-1} \mathbf{r}_d \tag{38c}$$

where $\hat{\mathbf{d}}_{ZF-sc}$, $\hat{\mathbf{d}}_{ZF-mc}$, and $\hat{\mathbf{d}}'_{ZF-mc}$ a the recovered data according to ZF-BLE for users of single cell and scenarios one and two of multi-cell, respectively, and \mathbf{R}_n is a $(NQ + W - 1) \times (NQ + W - 1)$ covariance matrix of the noise. When the noise is temporally uncorrelated, $\mathbf{R}_n = \sigma^2 \mathbf{I}_{NQ+W-1}$, the ZF-BLE equations become,

$$\hat{\mathbf{d}}_{ZF-sc} = (\mathbf{A}_{sc}^H \mathbf{A}_{sc})^{-1} \mathbf{A}_{sc}^H \mathbf{r}_d \tag{39a}$$

$$\hat{\mathbf{d}}_{ZF-mc} = (\mathbf{A}_{mc}^H \mathbf{A}_{mc})^{-1} \mathbf{A}_{mc}^H \mathbf{r}_d \tag{39b}$$

$$\hat{\mathbf{d}}'_{ZF-mc} = (\mathbf{A}'_{mc}{}^H \mathbf{A}'_{mc})^{-1} \mathbf{A}'_{mc}{}^H \mathbf{r}_d \tag{39c}$$

ZF-BLE completely eliminates MAI and ISI; however, it is similar to the LS channel estimator in that it amplifies the noise. This problem is overcome by MMSE-BLE and the detected data are [11],

$$\hat{\mathbf{d}}_{MMSE-sc} = (\mathbf{A}_{sc}^H \mathbf{R}_n^{-1} \mathbf{A}_{sc} + \mathbf{R}_d^{-1})^{-1} \mathbf{A}_{sc}^H \mathbf{R}_n^{-1} \mathbf{r}_d \tag{40a}$$

$$\hat{\mathbf{d}}_{MMSE-mc} = (\mathbf{A}_{mc}^H \mathbf{R}_n^{-1} \mathbf{A}_{mc} + \mathbf{R}_d^{-1})^{-1} \mathbf{A}_{mc}^H \mathbf{R}_n^{-1} \mathbf{r}_d \tag{40b}$$

$$\hat{\mathbf{d}}'_{MMSE-mc} = (\mathbf{A}'_{mc}{}^H \mathbf{R}_n^{-1} \mathbf{A}'_{mc} + \mathbf{R}_d^{-1})^{-1} \mathbf{A}'_{mc}{}^H \mathbf{R}_n^{-1} \mathbf{r}_d \tag{40c}$$

where $\hat{\mathbf{d}}_{MMSE-sc}$, $\hat{\mathbf{d}}_{MMSE-mc}$, and $\hat{\mathbf{d}}'_{MMSE-mc}$ are the MMSE-BLE recovered data for users of single cell and scenarios one and two of multi-cell, respectively, and \mathbf{R}_d defined in (41) and represents a $KN \times KN$ covariance matrix of the users' data.

$$\mathbf{R}_d = \begin{bmatrix} E\{\mathbf{d}_1 \mathbf{d}_1^H\} & E\{\mathbf{d}_1 \mathbf{d}_2^H\} & \cdots & E\{\mathbf{d}_1 \mathbf{d}_K^H\} \\ E\{\mathbf{d}_2 \mathbf{d}_1^H\} & E\{\mathbf{d}_2 \mathbf{d}_2^H\} & \cdots & E\{\mathbf{d}_2 \mathbf{d}_K^H\} \\ \vdots & \vdots & \ddots & \vdots \\ E\{\mathbf{d}_K \mathbf{d}_1^H\} & E\{\mathbf{d}_K \mathbf{d}_2^H\} & \cdots & E\{\mathbf{d}_K \mathbf{d}_K^H\} \end{bmatrix} \tag{41}$$

Suppose that data symbols of different users are uncorrelated and normalized to have unity power, i.e., $\mathbf{R}_d = \mathbf{I}_{KN}$. Also, for uncorrelated noise $\mathbf{R}_n = \sigma^2 \mathbf{I}_{NQ+W-1}$. Thus, (39) will be,

$$\hat{\mathbf{d}}_{MMSE-sc} = (\mathbf{A}_{sc}^H \mathbf{A}_{sc} + \sigma^2 \mathbf{I})^{-1} \mathbf{A}_{sc}^H \mathbf{r}_d \tag{42a}$$

$$\hat{\mathbf{d}}_{MMSE-mc} = (\mathbf{A}_{mc}^H \mathbf{A}_{mc} + \sigma^2 \mathbf{I})^{-1} \mathbf{A}_{mc}^H \mathbf{r}_d \tag{42b}$$

$$\hat{\mathbf{d}}'_{MMSE-mc} = (\mathbf{A}'_{mc}{}^H \mathbf{A}'_{mc} + \sigma^2 \mathbf{I})^{-1} \mathbf{A}'_{mc}{}^H \mathbf{r}_d \tag{42c}$$

The noise variance can be estimated from (7) after the estimation of the total channel. It should be mentioned that the prescribed equalizers are followed by the hard detector for recovering QPSK symbols.

6 Simulation results

The TD-SCDMA parameters used in our simulations are listed in Table 1. Two scenarios of propagation channels are considered and their parameters are chosen from ITU recommendation for vehicular A and Indoor B channels as listed in Table 2 [13]. It is considered that the physical

channel is Rayleigh faded with AWGN of zero mean and σ^2 variance. It is assumed that the active and interfering users are transmitting data in the uplink direction and each user encounters a specified channel different from other users' channels.

The value of SIR equals to -12 dB in our simulations, to test the proposed method under worst interference situation and compare the performance with conventional estimators. This ratio is cumulative from the neighboring cells with

Table 1 Simulation parameters of the TD-SCDMA system

Chip rate	1.28 Mbps
Carrier frequency	1.95 GHz
Modulation	QPSK
RRC roll-off factor	0.22
Interfering users (K_2)	4 users
Effective training sequence length (P)	128 chips
Spreading factor (Q_K)	16 for each user
Data symbols per block per user	22 symbols

different power distribution, the users of the first cell construct 50 % from this ratio while the second and third neighboring cells have 30 and 20 % respectively from the interference ratio. Note that the spacing of paths in Indoor B channel is smaller than the chip period of 781 ns. This means that those paths are correlated and don't provide as much information as non-correlated paths. On contrary Vehicular A channel has three from six paths are higher than the chip period. Therefore the number of the estimated parameters (or information) will be increasing compared with indoor B channel. The first two simulations (Figs. 3, 4) show the three dimensional plots of the individual channel impulse response (CIR) of the transmitted active along the memory length (W) for the eight users. For comparison, we calculated the individual CIR for each two users, user 1, 2 across multi-cell rank 1 case 1 estimator, user 3,4 across multi-cell rank 2 case 2 and so on as referred in Fig. 3. Also, in Fig. 4, a different individual CIR's are listed with different approaches of estimators. From these figures, we can note the reduced rank technique with rank 1 has the least effect value at the same tap of the channel.

Table 2 Indoor and Vehicular channels parameters

Number of paths	Indoor B channel		Vehicular A channel	
	Speed of 3 km/h		Speed of 120 km/h	
	Relative delay (ns)	Relative mean power (dB)	Relative delay (ns)	Relative mean power (dB)
Path 1	0	0	0	0
Path 2	100	-3.6	310	-1
Path 3	200	-7.2	710	-9
Path 4	300	-10.8	1,090	-10
Path 5	500	-18	1,730	-15
Path 6	700	-25.2	2,510	-20

Fig. 3 CIR with different channel estimators, according to indoor channel

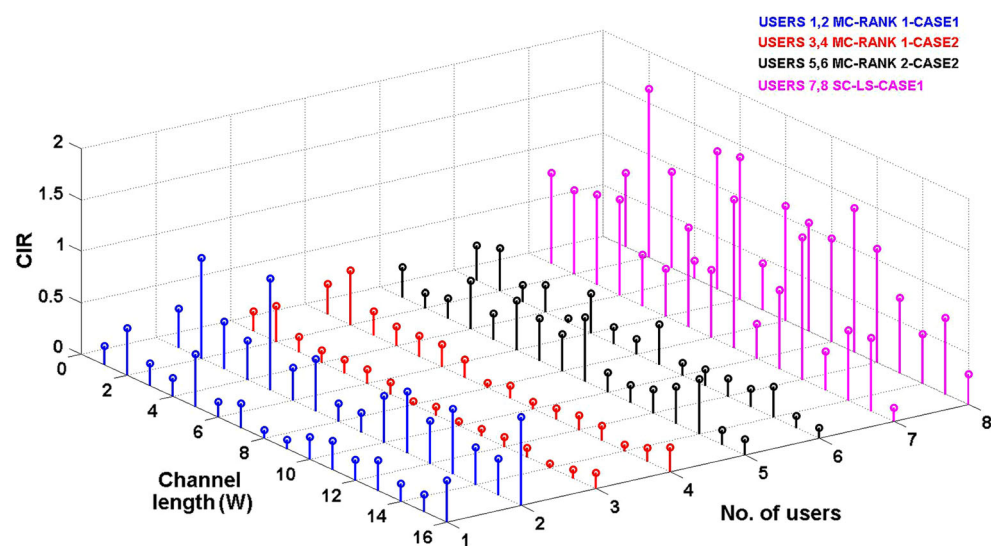


Fig. 4 CIR with different channel estimators, according to vehicular channel

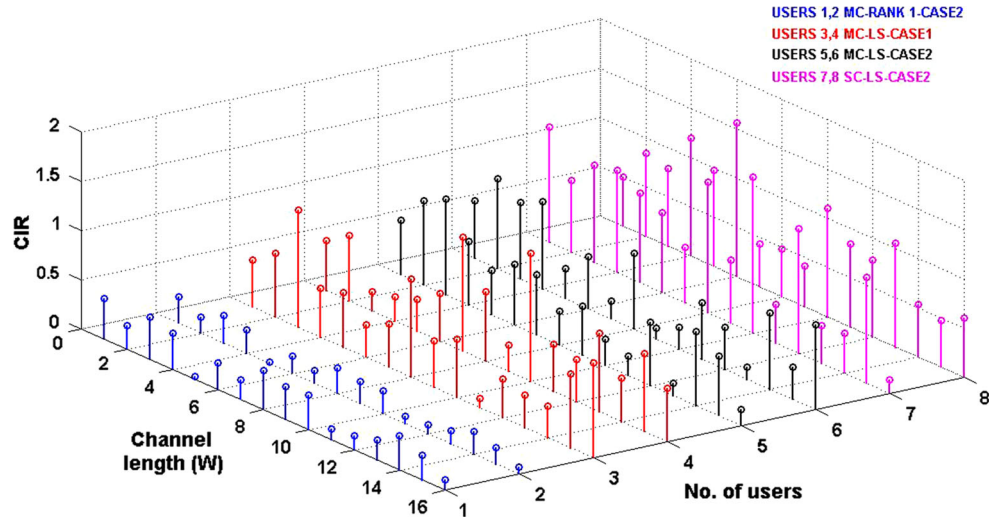


Fig. 5 Normalized MSE versus SNR in dB with (SIR = -12 dB) for indoor channel

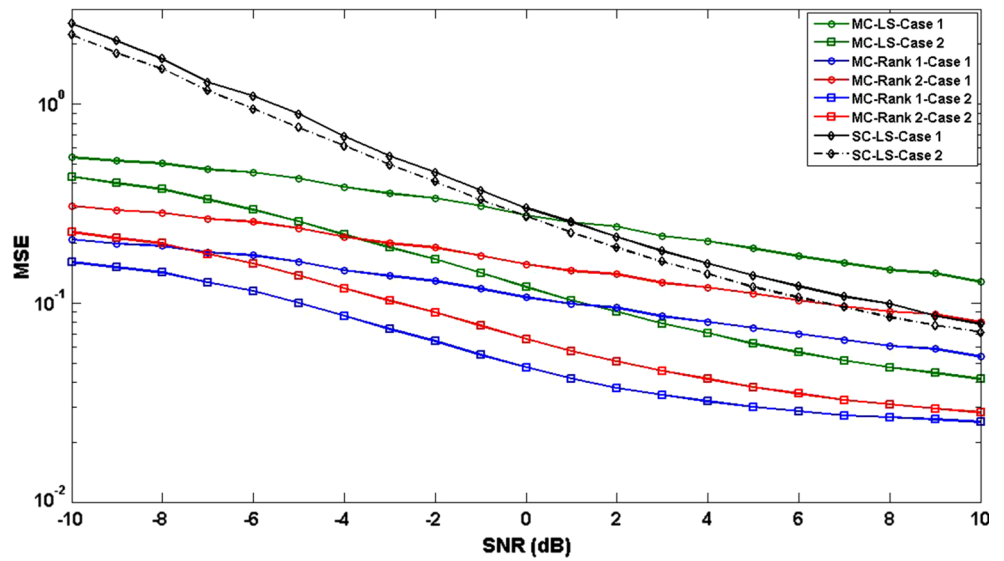
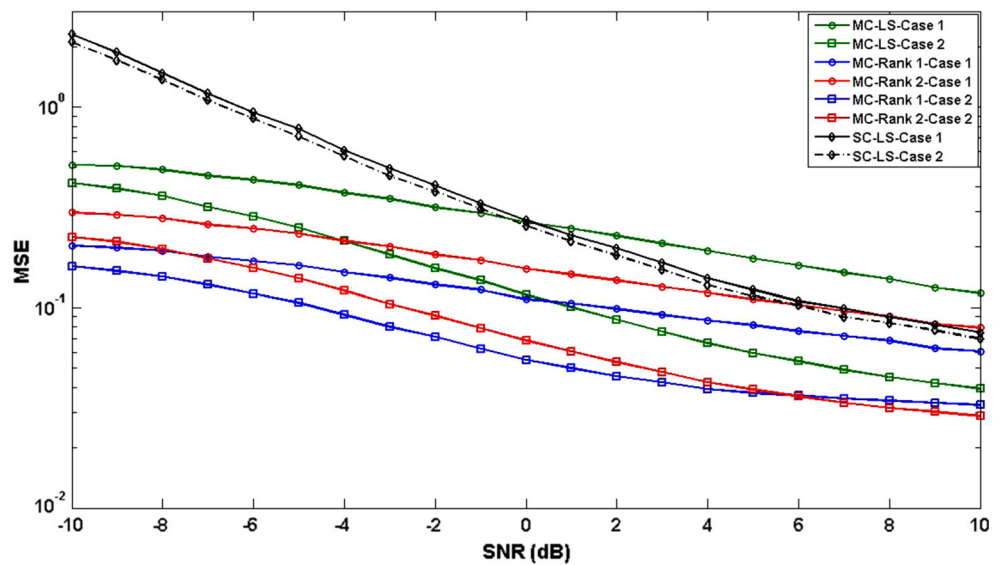


Fig. 6 Normalized MSE versus SNR in dB with (SIR = -12 dB) for vehicular channel



The second group of simulations (Figs. 5, 6) show the performance of normalized Mean Square Error (MSE) versus bit energy to noise spectral density, E_b/N_o , in dB and These simulations are averaged by transmitted 2000 independent bursts for each proposed user. In this paper, the proposed estimators are case one of multi-cell using LS algorithm with four active and 4 interfering users, reduced rank with rank one and two for case one, case two of multi-cell using LS algorithm with eight active and four interfering users, reduced rank with rank one and two of case two, and single cell using LS. These figures (Figs. 5, 6) compares the simulations for the MSE on the channels Indoor B and vehicular A respectively. Generally, the channel estimators based multi-cell strategy outperforms estimators based serving or single cell processing. It is noticed also that at the low SNR the reduced rank

estimators are the preferred solution as they have the least number of unknowns to be estimated, in addition introduce a low error performance. For large SNR the SC estimators become more enhanced and their performance closed to the LS and Rank 2 estimators especially in case one. A passing insight to the mentioned simulation plots shows the existence and validity of reduced rank technique. And rank one estimator has the superiority over the other estimator; it has improvement by -10 and -12.6 dB in low SNR of indoor channel over the single cell LS estimator for case 1 and case 2 respectively. As a general behavior, case two of multi-cell is still dominant and it also preceding case one of multi-cell.

Another set of simulations are aimed to show the accuracy of the estimators performance via the correlation coefficient measure, where this simulations introduced the

Fig. 7 The correlation coefficient versus SNR in dB with (SIR = -12 dB)

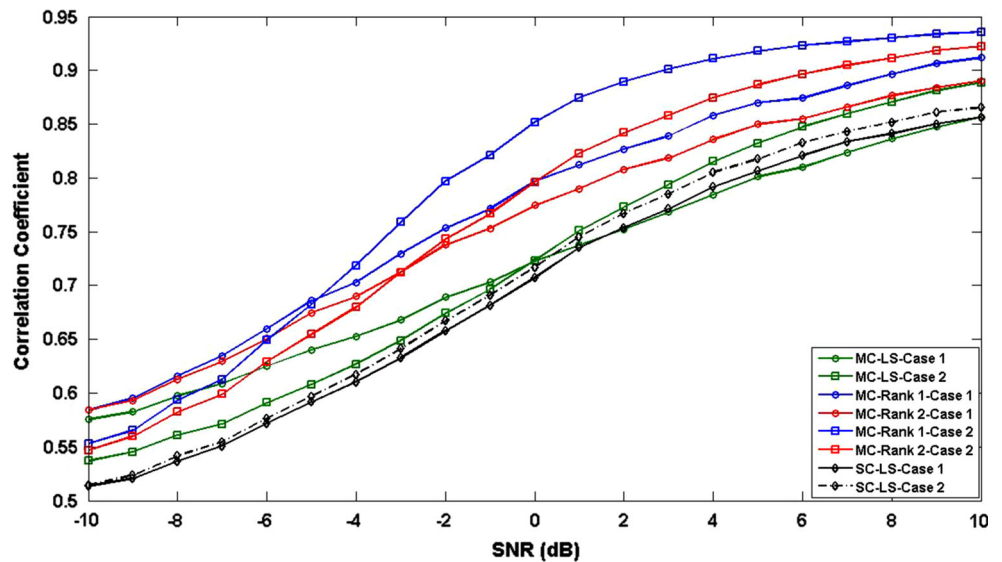
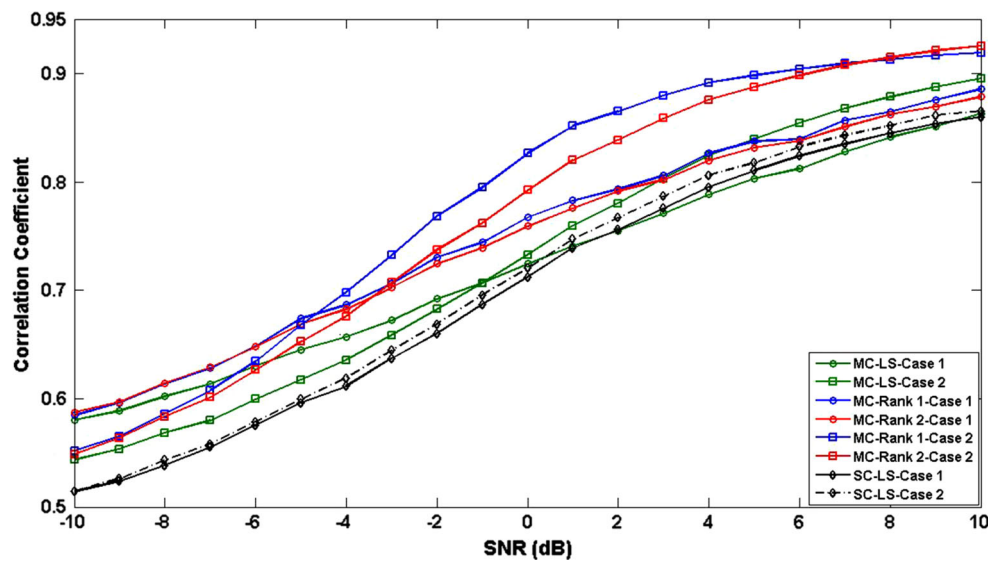


Fig. 8 The correlation coefficient versus SNR in dB with (SIR = -12 dB)



similarity between the ideal CIR and estimated CIR. Figure 7 demonstrates the statistical results of the correlation coefficient under the Indoor B channel specification. The simulations result shows that the rank one estimator has the highest correlation coefficient. Figure 8 shows the results of tests of the channel estimation accuracy under Vehicular A channel. The highest correlation coefficient values varied among the rank one and rank two along the SNR axis. For the case two, below 7 dB, the rank one has the leading rank over the estimators. Above 2 dB, rank two and rank three outperform rank one.

Finally, the performance of Bit Error Rate (BER) versus E_b/N_o in dB has been tested for the following data detectors: MMSE-BLE for single cell, MMSE-BLE for case one of multi-cell with four active and four interfering users, MMSE-BLE for reduced rank of case one with rank one and two,

MMSE-BLE for case two of multi-cell with eight active and four interfering users, and MMSE-BLE for reduced rank of case two with rank one and two. The data simulations re averaged over 4,000 independent transmitted bursts. A comparison of the BER performance of the full rank conventional based detectors (LS case 1 and case 2) and the reduced rank based detectors is drawn for both Indoor (see Fig. 9) and vehicular (see Fig. 10) channels. In Fig. 9, Rank one based detector behaves always better than the other detectors and it introduces improvement about 6.4 dB for case 1 and 9 dB for case 2 gained over MMSE-LS and MMSE-post processing detectors for the indoor channel. While, the improvement of rank two based detectors are about 5 dB for case 1 and 7 dB for case 2 lower than MMSE-LS and MMSE-post processing detectors. In Fig. 10, for the vehicular channel, the detectors

Fig. 9 BER versus SNR in dB with (SIR = -12 dB) for indoor channel

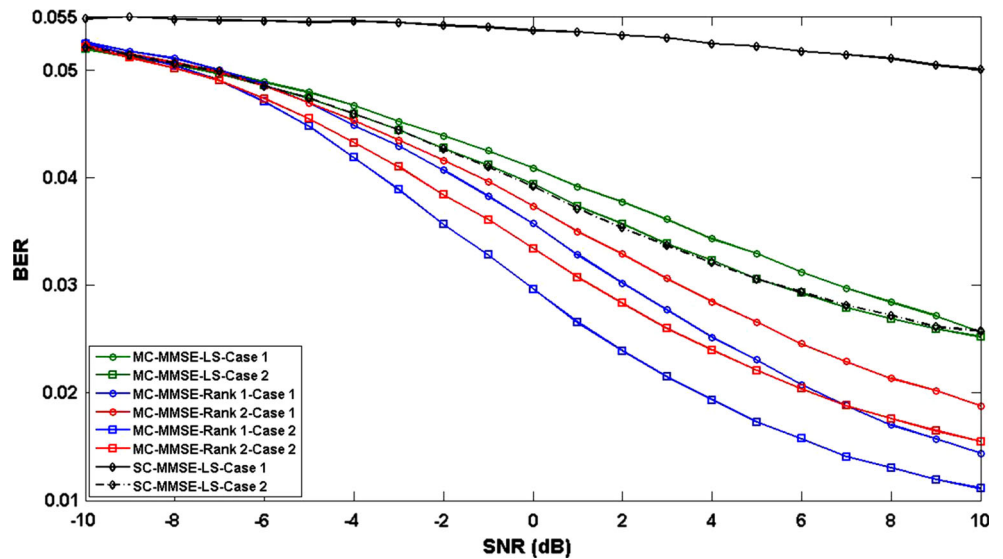
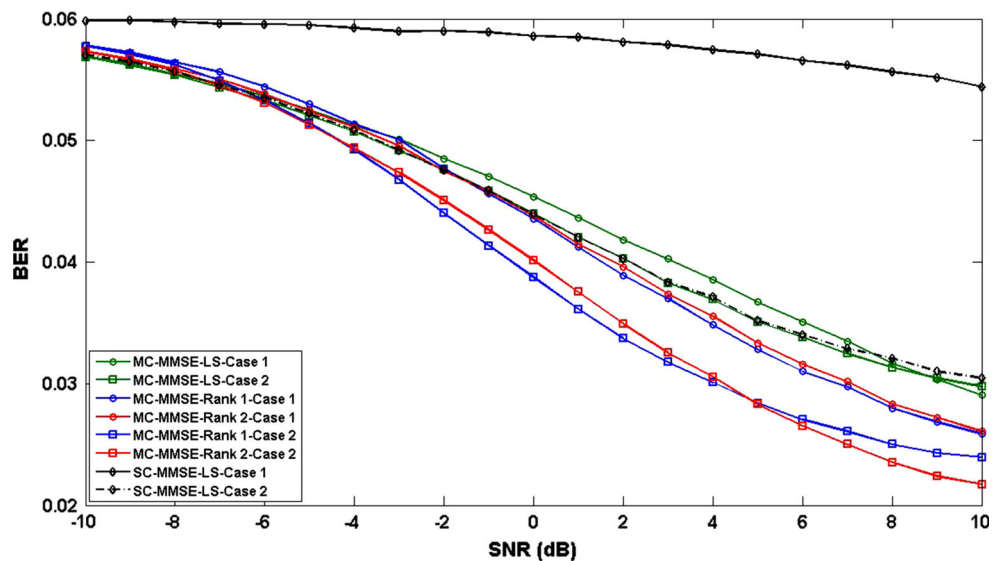


Fig. 10 BER versus SNR in dB with (SIR = -12 dB) for vehicular channel



that based on reduced rank channel estimators exhibits good performance and rank one and rank two have the best behaviors in the first and second cases. 3 dB is gained for rank one and rank two based detector in case 1 and 6 dB is gained for rank one and rank two based detector in case 2. Now, without any adopt, the reduced rank technique can introduce a significant improvement to the TD-SCDMA systems and their applications.

7 Conclusion

In this paper, a new technique called the SVD technique has been considered for channel estimation methods at TD-SCDMA that is based on reducing the rank order of the channel system matrix. This technique is implemented for the multi-cell model of channel estimations and tested for multi-user joint detection and it involves detecting the active users of the serving cell as well as the neighboring interfering users. In addition, the SVD technique is adopted for achieving the reduced ranking of the system channel matrix. It is seen that the new technique offer superior performance over the traditional ones in single-cell and multi-cell models. Thus, the new technique improves the performance of the TD-SCDMA system with low rank processing and low computation complexity.

References

- Liu, G., Zhang, J., Zhang, P., Wang, Y., Liu, X., & Li, S. (2006). Evolution map from TD-SCDMA to future B3G TDD. *IEEE Communications Magazine*, pp. 54–61.
- Peng, M., Wang, W., & Chen, H.-H. (2010). TD-SCDMA evolution. *IEEE Vehicular Technology Magazine*, 5(2), 28–41.
- Shao-li, K., Zhang-ding, Q., & Shi-he, L. (2001). The effect of channel estimation Errors on joint detection algorithms in TD-SCDMA system. *Proc. IEEE-ICII'2001*, p. 303.
- Song, X., Li, K., & Hu, A. (2007). Two-stage channel estimation algorithm for TD-SCDMA system employing multi-cell joint detection. *Circuit System Signal Processing*, 26(6), 76–80.
- Steiner, B., Jung, P. (1994). Optimum and suboptimum channel estimation for the uplink of CDMA mobile radio systems with joint detection. *European Trans. Telecommunications Related Techniques*, pp. 39–50.
- Zhang, X., Wang, W., Chen, S., & Wang, C. (2010). Multi-cell channel estimation and multi-cell joint detection in TD-SCDMA system. *Proc. IEEE-WCNIS'2010*, p. 130.
- Scharf, L. L. (1991). The SVD and reduced rank signal processing. *Signal Processing*, 25(2), 113–133.
- Hua, Y., Nikpour, M., & Stoica, P. (2001). Optimal reduced-rank estimation and filtering. *IEEE Transactions on Signal Processing*, 49(3), 457–469.
- 3GPP TS 25.223, V9.0.0. (2009). Technical specification group radio access network; spreading and modulation (TDD). Dec. 2009.
- 3GPP TS 25.102, V10.0.0. (2010). User equipment (UE) radio transmission and reception (TDD). Dec. 2010.
- Zhaogan, L., Yuan, R., Taiyi, Z., & Wang, W. (2010). Multiuser MIMO OFDM based TDD/TDMA for next generation wireless communication systems. *Wireless Personal Communications*, 52(20), 289–324.
- Chitrapu, P., & Brianncon, A. (2004). *Wideband TDD, WCDMA for the unpaired spectrum*. England: Wiley.
- M.1225 ITU-R Recommendation M.1225. (1997). Guidelines for evaluation of radio transmission technologies for IMT-2000.
- 3GPP TS 25.221, V7.4.0. (2007). Physical channels and mapping of transport channels onto physical channels (TDD). Sept. 2007.

Author Biographies



Ali K. Marzook is received the B.Sc. (1999) in Electrical Engineering and Postgraduate Higher Diploma (2001) and M.Sc. (2004) degrees in Communication Engineering from the University Of Basrah in Iraq. Since November 2002, he has been a lecturer in the University of Basrah, Iraq. From July 2008 joined the University of Putra Malaysia (UPM) to have Ph.D. degree in Computer and Communications Networks Engineering. Research areas are

Mobile communications and wireless technology, radio access techniques and space–time signal processing.



Alyani received her B.Eng. (Hons) from the University of Huddersfield, in 1999, her M.Sc., and Ph.D. from the University of Birmingham, in 2001 and 2006. She subsequently became a lecturer in Universiti Putra Malaysia in 2006 and now works as an Associate Professor. She has been appointed to various administrative positions—Deputy Director of Centre for Academic Development, 2012—now and Head of Department of Computer and Communication Systems Engineering, 2010–Feb 2012. Alyani is an active member on IEEE since 2006 and she serves as an Executive Committee for IEEE AP/MTT/EMC Chapter. Alyani specializes in the development of RF and microwave devices particularly passive filters, antennas and sensors. In recognition of her contributions in research, Alyani has been awarded the Young Excellent Researcher Award for 2010 by the university.



Borhanuddin received his B.Sc.(Hons) from Loughborough University of Technology in 1979, his M.Sc., and Ph.D. from the University of Wales (Cardiff), in 1981 and 1985, respectively and subsequently became a lecturer in Universiti Putra Malaysia since 1985. He served the university at various administrative positions—Director of the Institute of Multimedia and Software, 2002–2006; Director of Institute of Advanced Technology UPM (ITMA), and Direc-

tor of the National Centre of Excellence in Sensor Technology (NEST). In 1996 he helped to realize the formation of Teman project a precursor to MYREN, and later was made the Chairman of the MYREN Research Community till 2006. He is a Chartered Electrical Engineer and a member of IET and Senior Member of IEEE. He was Chair of IEEE Malaysia Section 2002–2004, and ComSoc Chapter twice, 1999–2002, and 2006–2008, and is serving in ComSoc AP Board and IEEE Region 10. His research interest spans wireless communications in particular wireless sensor networks and broadband communications. He has authored and co authored some 100 journal papers and 200 conference papers under those areas of interests.



Aduwati Sali is currently a Lecturer at Department of Computer and Communication Systems, Faculty of Engineering, Universiti Putra Malaysia (UPM) since July 2003. She obtained her Ph.D. in Mobile Satellite Communications from University of Surrey, UK, in July 2009, her M.Sc., in Communications and Network Engineering from UPM in April 2002 and her B.Eng. in Electrical Electronics Engineering (Communications) from University of Edinburgh in 1999.

She worked as an Assistant Manager with Telekom Malaysia Bhd

from 1999 until 2000. She involved with EU-IST Satellite Network of Excellence (SatNex) I & II from 2004 until 2009. Since then, she is the principle investigator for projects under the funding bodies Malaysian Ministry of Science, Technology and Innovation (MOSTI), Research University Grant Scheme (RUGS) UPM and The Academy of Sciences for the Developing World (TWAS-COMSTECH) Joint Grants. Her research interests are radio resource management, MAC layer protocols, satellite communications, wireless sensor networks, disaster management applications, 3D video transmissions.



Sabira Khatun is received B.Sc.(Hons), M.Sc., in applied mathematics and PhD in computational algorithm from University of Rajshahi, Bangladesh in 1987, 1990 and 1994 respectively. She received a second Ph.D. in Communication and Network Engineering from University Putra Malaysia in 2003. Currently, she is working as professor in the Department of Computer Systems and Networks, Faculty of Computer Systems and Software Engineer-

ing, University Malaysia Pahang, Malaysia. Her research interests include wireless communications & networks, digital signal processing, UWB and biomedical applications. Prof Khatun is an active member of IEEE since 2007. She is also members of IEEE Communication Society, IEEE Microwave Theory and Techniques Society, Fellow member of International Association of Computer Science and Information Technology (IACSIT) and IEEE Women in Engineering.